doi:10.1093/jmcb/mjw035
Published online July 19, 2016

Article

Prostaglandin E2 receptor EP3 regulates both adipogenesis and lipolysis in mouse white adipose tissue

Hu Xu[1,†], Jia-Lin Fu[1,†], Yi-Fei Miao[2], Chun-Jiong Wang[1], Qi-Fei Han[1], Sha Li[1], Shi-Zheng Huang[1], Sheng-Nan Du[1], Yu-Xiang Qiu[1], Ji-Chun Yang[1], Jan-Åke Gustafsson[2], Richard M. Breyer[3], Feng Zheng[4], Nan-Ping Wang[4], Xiao-Yan Zhang[4,5], and You-Fei Guan[1,4,*]

[1] Department of Physiology and Pathophysiology, School of Basic Medical Sciences, Peking University Health Science Center, Beijing 100191, China
[2] Center for Nuclear Receptors and Cell Signaling, Department of Biology and Biochemistry, University of Houston, Houston, TX 77204, USA
[3] Department of Veterans Affairs, Tennessee Valley Health Authority, and Department of Medicine, Vanderbilt University Medical Center, Nashville, TN 37232, USA
[4] Advanced Institute for Medical Sciences, Dalian Medical University, Dalian 116044, China
[5] Department of Physiology, AstraZeneca–Shenzhen University Joint Institute of Nephrology, Shenzhen University Health Science Center, Shenzhen 518060, China
[†] These authors contributed equally to this work.
* Correspondence to: You-Fei Guan, E-mail: guanyf@dmu.edu.cn

Among the four prostaglandin E2 receptors, EP3 receptor is the one most abundantly expressed in white adipose tissue (WAT). The mouse *EP3* gene gives rise to three isoforms, namely EP3α, EP3β, and EP3γ, which differ only at their C-terminal tails. To date, functions of EP3 receptor and its isoforms in WAT remain incompletely characterized. In this study, we found that the expression of all EP3 isoforms were downregulated in WAT of both db/db and high-fat diet-induced obese mice. Genetic ablation of three EP3 receptor isoforms ($EP3^{-/-}$ mice) or EP3α and EP3γ isoforms with EP3β intact (EP3β mice) led to an obese phenotype with increased food intake, decreased motor activity, reduced insulin sensitivity, and elevated serum triglycerides. Since the differentiation of preadipocytes and mouse embryonic fibroblasts to adipocytes was markedly facilitated by either pharmacological blockade or genetic deletion/inhibition of EP3 receptor via the cAMP/PKA/PPARγ pathway, increased adipogenesis may contribute to obesity in $EP3^{-/-}$ and EP3β mice. Moreover, both $EP3^{-/-}$ and EP3β mice had increased lipolysis in WAT mainly due to the activated cAMP/PKA/hormone-sensitive lipase pathway. Taken together, our findings suggest that EP3 receptor and its α and γ isoforms are involved in both adipogenesis and lipolysis and influence food intake, serum lipid levels, and insulin sensitivity.

Keywords: arachidonic acid, EP3 receptor isoform, PKA, PPARγ, insulin resistance, obesity

Introduction

Obesity has become a major health concern and an important social problem worldwide. It is associated with the development of a number of metabolic and cardiovascular disorders including insulin resistance, Type 2 diabetes, fatty liver disease, hypertension, and atherosclerosis. Overgrowth of white adipose tissue (WAT), a major tissue involved in energy homeostasis due to enhanced differentiation and proliferation of white adipocyte progenitors is directly related to the prevalence of obesity (Bays, 2014). Recently, increasing evidence has demonstrated that adipose tissues are heterogenic (Sanchez-Gurmaches and Guertin, 2014; Dempersmier and Sul, 2015) and include three major types, namely white, brown, and beige adipocytes. In general, white adipocytes store the excess energy as triglycerides (TG) and hydrolyze TG into free fatty acids (FFAs) and glycerol in the circulation during fasting, while brown and beige adipocytes dissipate energy into heat (Ahmadian et al., 2010). All adipocytes are differentiated from preadipocytes. This process is called adipogenesis and characterized by the development of an adipocyte phenotype and the accumulation of TG in lipid droplets. Adipogenesis is initiated by extracellular and intracellular factors controlled by peroxisome proliferator-activated receptor γ (PPARγ) and CCAAT-enhancer-binding proteins (C/EBPs). In addition, cyclic AMP (cAMP) response element-binding protein

Received October 21, 2015. Revised March 29, 2016. Accepted April 4, 2016.

(CREB) is a vital transcription factor that functions at the early stage in adipogenesis to promote the expression of PPARγ and C/EBPα (Gustafson et al., 2015).

Lipolysis often coincides with obesity, as previously shown by many research groups (Langin et al., 2005; Langin and Arner, 2006; Ryden and Arner, 2007; Lafontan and Langin, 2009). This process breaks down TG into glycerol and FFAs using a few lipases. Adipose triglyceride lipase (ATGL) cleaves TG into diacylglycerol, and hormone-sensitive lipase (HSL) continues this process, which is completed by monoglyceride lipase (MGL) (Ahmadian et al., 2010). Intracellular cAMP activates protein kinase A (PKA), which phosphorylates HSL at Ser660 to activate it and phosphorylates perilipin A, an important lipid droplet-coating protein. Phosphorylation of perilipin A allows ATGL/HSL to translocate to the lipid droplet surface to hydrolyze TG stored in lipid droplets (Ahmadian et al., 2010). It has been previously documented that lipolysis process is also regulated by PPARγ, as supported by the fact that expression of ATGL and HSL is under the control of PPARγ (McTernan et al., 2002; Kershaw et al., 2007). When excessive FFAs enter circulation, it may result in ectopic lipid deposition, hyperlipidemia, and impaired insulin sensitivity (Arner and Langin, 2014; Wang et al., 2014a, b).

Prostaglandin E2 (PGE2) is the predominant prostaglandin produced in WAT. As an important lipid mediator, PGE2 may play a crucial role in the regulation of adipose functions and development of obesity (Kimple et al., 2014). PGE2 biosynthesis involves multiple enzymatic steps and requires the sequential action of phospholipase A2 (PLA2), cyclooxygenases (COX-1 and COX-2), and PGE synthases (mPGES-1, mPGES-2, and cPGES). PGE2 exerts its biological effects by acting on its four receptors (EP1, EP2, EP3, and EP4), all of which are G protein-coupled receptors. Each PGE2 receptor is coupled to different intracellular signaling pathways. As a Gq protein-coupled receptor, EP1 could raise Ca^{2+} concentration in response to PGE2 treatment or under pharmacological stimulation. Activation of EP2 and EP4 increases intracellular cAMP levels via the Gs protein-coupled signaling pathway. Unlike the other three EP receptors, EP3 has three isoforms in mice, namely EP3α, EP3β, and EP3γ, which are derived from alternating splicing of a single *EP3* gene and differ in their C-terminal tail sequences (Supplementary Figure S1A). In general, EP3 receptor couples to the Gi protein to decrease intracellular cAMP concentration by inhibiting adenylyl cyclase. However, the detailed function and signaling transduction for each isoform remain poorly understood (Sugimoto and Narumiya, 2007). Increasing evidence demonstrates that PGE2 and its synthesizing enzymes play an important role in adipose tissues, likely affecting both adipogenic and lipolytic processes (Fain et al., 2000; Fujimori et al., 2014; Garcia-Alonso and Claria, 2014). It was reported that a marked reduction of adipose PGE2 through deletion of adipocyte-specific phospholipase A (AdPLA) led to a higher rate of lipolysis, reduced adipose tissue mass, and resistance to diet-induced obesity (DIO), mainly due to increased cAMP levels and probably decreased activation of Gi-coupled EP3 receptor (Strong et al., 1992; Jaworski et al., 2009). A recent study further showed that deletion of all EP3 isoforms in mice resulted in obese and insulin resistant phenotypes. The loss of hypothalamic PGE2 signaling and peripheral EP3 receptor-mediated PGE2 actions has been proposed as the causes for obesity in EP3-null mice (Sanchez-Alavez et al., 2007). However, the underlying molecular mechanisms and the roles of EP3 receptor and its isoforms in WAT remain largely unexplored.

In the present study, we report that genetic deletion of all three EP3 receptor isoforms ($EP3^{-/-}$ mice) or EP3α and EP3γ isoforms with EP3β left (EP3β mice), facilitates adipogenesis via the cAMP/PKA/PPARγ pathway, resulting in an obese phenotype. Meanwhile, increased lipolysis due to the activation of PKA in WAT of $EP3^{-/-}$ and EP3β mice leads to hyperlipidemia and insulin resistance. Altogether, our findings indicate that EP3 receptor and its α and γ isoforms are involved in the regulation of both adipogenesis and lipolysis.

Results

Expression of EP3 receptor in WAT of normal and obese mice

As previously reported (Borglum et al., 1999), mouse EP3 receptor is widely expressed in various tissues, among which WAT has high-level expression (Figure 1A). In both db/db and high-fat DIO models, the mRNA and protein levels of EP3 receptor in WAT were significantly reduced (Figure 1B–E).

Mice with genetic deletion of all three EP3 receptor isoforms ($EP3^{-/-}$) or EP3α and EP3γ isoforms (EP3β) displayed an obese phenotype

In $EP3^{-/-}$ mice with all three EP3 isoforms genetically deleted, mRNA expression of entire EP3 receptor was almost completely abolished, with no changes in EP1, EP2, or EP4 expression (Supplementary Figure S1D). However, in EP3β mice where EP3α and EP3γ isoforms were deleted, although mRNA expression of EP3α and EP3γ isoforms were absent and total EP3 expression was significantly reduced, EP3β expression was markedly increased, with little change in the expression of EP1, EP2, and EP4 (Supplementary Figure S1E). In both $EP3^{-/-}$ and EP3β mice, a significant increase in body weight was observed compared with their wild-type (WT) littermates. However, the body weights were comparable between $EP3^{-/-}$ and EP3β mice (Figure 2A). To investigate whether the increase in body weight for both $EP3^{-/-}$ and EP3β mice was attributed to the altered fat content, a MRI analysis was performed. The analysis of body composition revealed significantly increased fat mass in both $EP3^{-/-}$ and EP3β mice (Figure 2B). Epididymal fat mass was significantly higher in $EP3^{-/-}$ and EP3β mice compared with their WT littermates (Supplementary Figure S2A). Sections of epididymal fat tissues showed that adipocyte size was significantly increased in both $EP3^{-/-}$ and EP3β mice (Figure 2C). In addition, for both $EP3^{-/-}$ and EP3β mice, the weight gain was associated with increased food intake (Supplementary Figure S2B) and reduced motor activities during both light and dark cycles (Figure 2D and E). Restriction of food intake to the amount comparable to WT mice for 2 weeks was sufficient to correct the obese phenotype and serum TG levels in $EP3^{-/-}$ and EP3β mice (Supplementary Figure S2C and D), suggesting a key role of increased food intake.

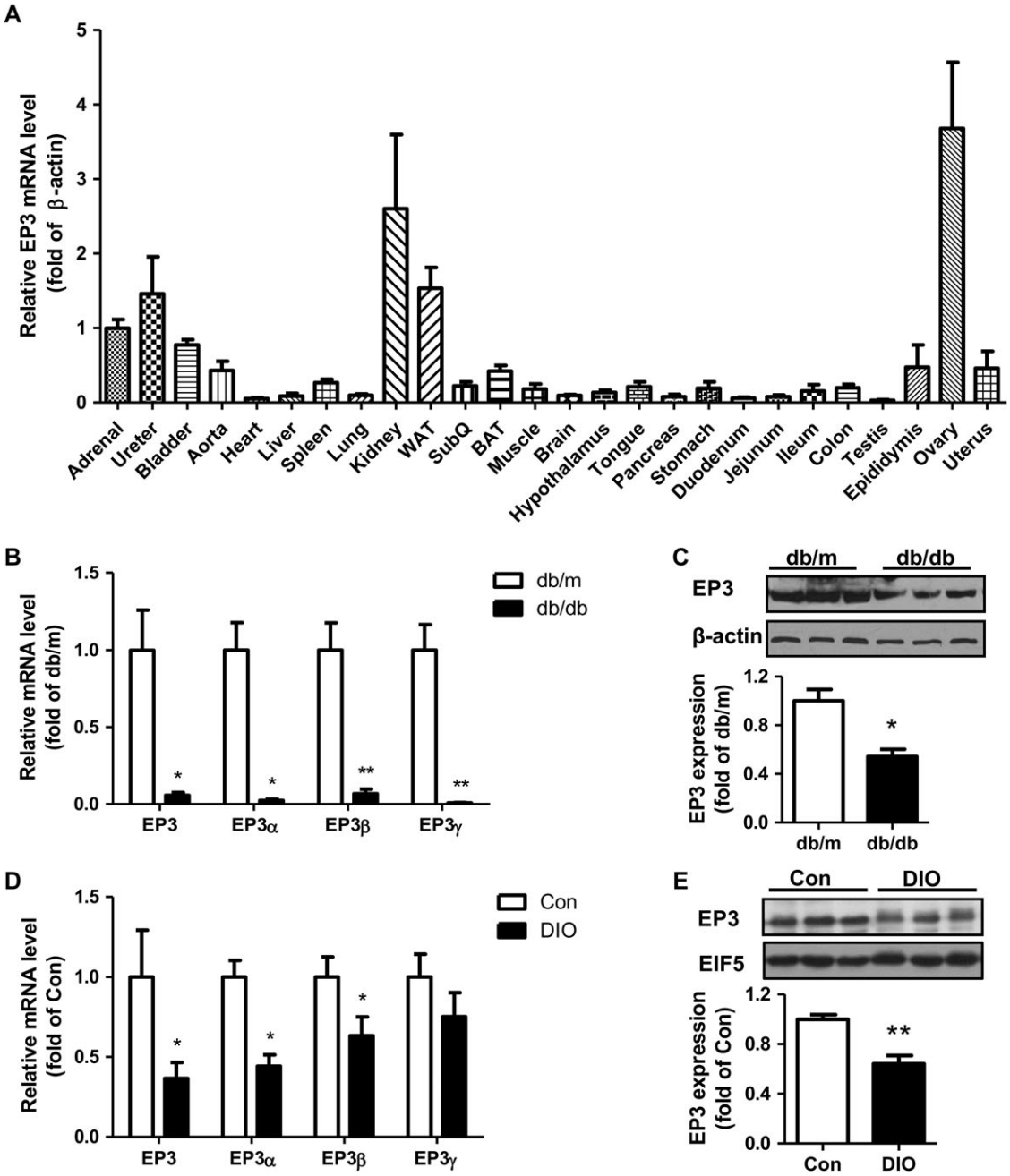

Figure 1 The expression of EP3 receptor in WAT. (**A**) EP3 expression in various organs and tissues of normal mice. Four male mice and four female mice were used to detect the mRNA levels of total EP3 in 26 organs and tissues by real-time PCR. (**B** and **C**) Decreased expression of EP3 receptor in WAT of db/db mice compared with db/m mice. mRNA level was quantified by real-time PCR (**B**, $n = 5$ in each group) and protein level was detected by western blot (**C**, $n = 3$ in each group). The lower bargraph in **C** is the quantification of western blot. (**D** and **E**) Decreased expression of EP3 receptor in WAT of DIO mice compared with control diet mice. mRNA level was quantified by real-time PCR (**D**, $n = 10$ in each group) and protein level was detected by western blot (**E**, $n = 4$ in each group). The lower bargraph in **E** is the quantification of western blot. $^*P < 0.05$, $^{**}P < 0.01$ vs. db/m mice (**B**, **C**) or control diet mice (**D**, **E**).

$EP3^{-/-}$ and EP3β mice exhibited insulin resistance and inflammation of WAT

Insulin resistance is frequently accompanied by obesity even though the causal relationship is unclear (Ye, 2013). Insulin tolerance test (ITT) and oral glucose tolerance test implied that both $EP3^{-/-}$ and EP3β mice at 8 weeks old were normal (data not shown). At 20 weeks when obese phenotype becames evident, $EP3^{-/-}$ mice developed moderate insulin resistance, as indicated by hyperinsulinemic-euglycemic clamp test (Figure 3A). ITT results also indicated that both $EP3^{-/-}$ and EP3β mice were

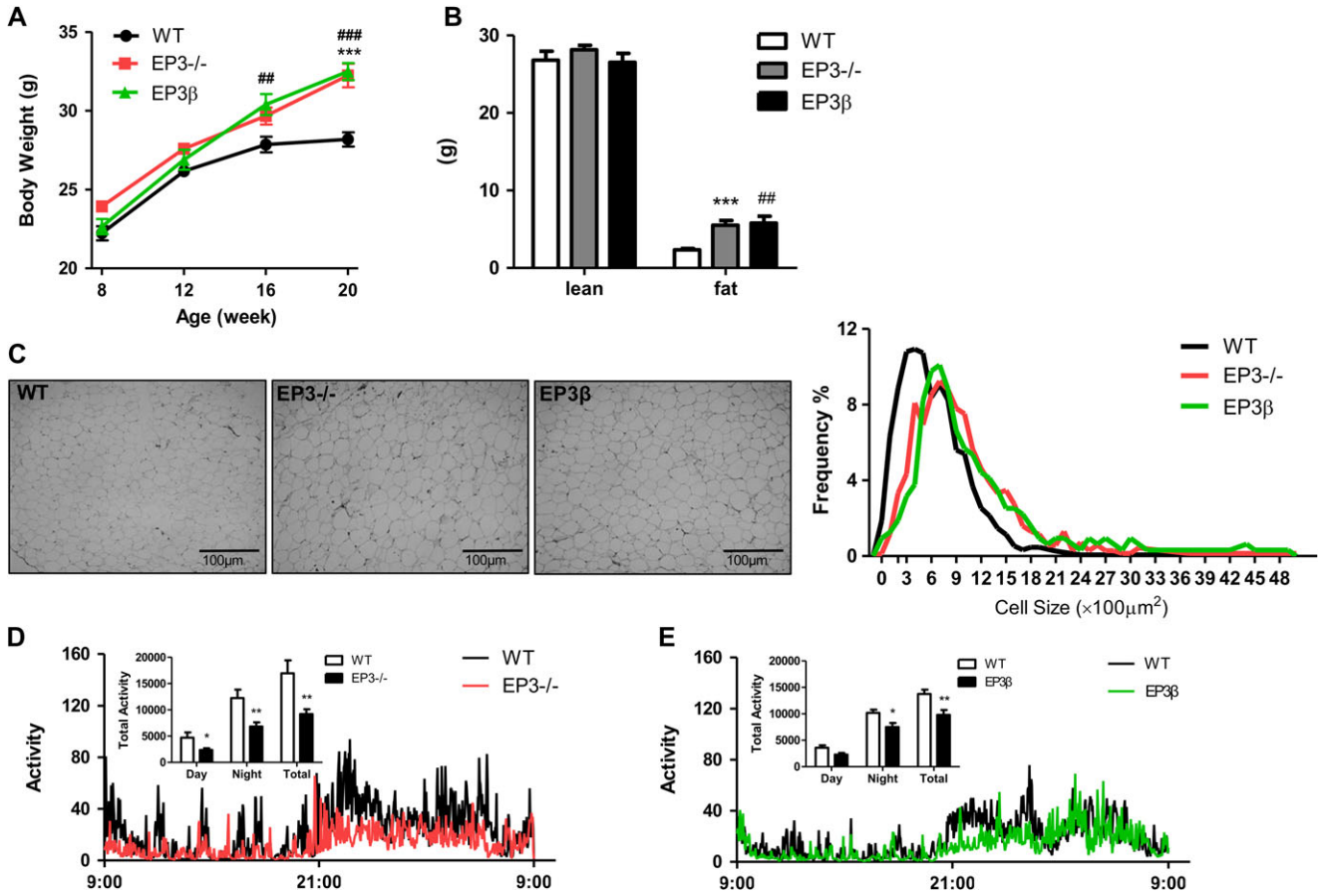

Figure 2 Both EP3$^{-/-}$ and EP3β mice displayed spontaneous obese phenotype. (**A**) Increased body weight of the EP3$^{-/-}$ and EP3β mice. The body weight of male EP3$^{-/-}$ mice (n = 6), EP3β mice (n = 13), and their WT littermates (n = 34) were measured from 8 to 20 weeks. (**B**) MRI analysis of the body composition of WT, EP3$^{-/-}$, and EP3β mice at 20 weeks. The lean mass and fat mass of WT (n = 6), EP3$^{-/-}$ (n = 7), and EP3β (n = 5) mice were analyzed. (**C**) Morphologic analysis of adipocytes from WAT of WT, EP3$^{-/-}$, and EP3β mice at 20 weeks. Representative pictures (400×) are shown on the left. The adipocyte size and the frequency of the cell size were calculated and shown on the right. Three sections from different mice per group were randomly selected. (**D** and **E**) Less motor activities in the EP3$^{-/-}$ and EP3β mice than in WT mice. Motor activities were measured by the metabolic cage for 24 h lasting one light and dark cycle. Accumulated activities were calculated during light time, dark time, and total time course as shown in inset. n = 12 for WT, n = 12 for EP3$^{-/-}$ mice, and n = 9 for EP3β mice. The mice were measured at the age of 4–6 months. *P < 0.05, **P < 0.01, ***P < 0.001, EP3$^{-/-}$ vs. WT mice; $^{\#}P$ < 0.05, $^{\#\#}P$ < 0.01, $^{\#\#\#}P$ < 0.001, EP3β vs. WT mice.

insulin resistant (Figure 3B and C). Although no difference in fasting blood glucose levels was observed among EP3$^{-/-}$ mice, EP3β mice, and their WT littermates (Figure 3D), serum insulin levels (Figure 3E), and homeostasis model of assessment-insulin resistance (HOMA-IR) index (Figure 3F) were significantly elevated in EP3$^{-/-}$ and EP3β mice, consistent with previous reports that the inhibition of EP3 accelerated insulin secretion (Kimple et al., 2013).

The serum TG and glycerol concentrations in EP3$^{-/-}$ and EP3β mice were increased at 8 weeks (Supplementary Figure S2C). Additionally, the VLDL-TG production in EP3$^{-/-}$ and EP3β mice was increased compared with WT mice, with TG clearance rate unchanged (Figure 3G and H). These findings suggest that high levels of TG may account for the impaired insulin sensitivity. Since inflammation in WAT is also an important factor that influences the insulin sensitivity, we examined phosphorylation of NF-κB p65 in WAT. The levels of phosphorylated NF-κB p65 were significantly elevated in WAT of EP3$^{-/-}$ and EP3β mice (Supplementary Figure S3A and B), suggesting increased NF-κB activities.

Activation of EP3 receptor suppressed adipogenesis

To characterize the mechanisms in the development of the obese phenotype in EP3$^{-/-}$ and EP3β mice, the role of EP3 receptor in preadipocyte proliferation and differentiation was determined. Activation or antagonism of EP3 receptor had little effect on cell viability and proliferation of 3T3-L1 preadipocytes and mouse embryonic fibroblasts (MEFs), as assessed by MTT assay (Supplementary Figure S4A). However, inhibition of endogenous PGE2 by indomethacin, an inhibitor of both COX-1 and COX-2, dramatically facilitated MEF differentiation (Figure 4A). On the contrary, treatment of PGE2 suppressed MEF differentiation in a dose-dependent manner (Figure 4B).

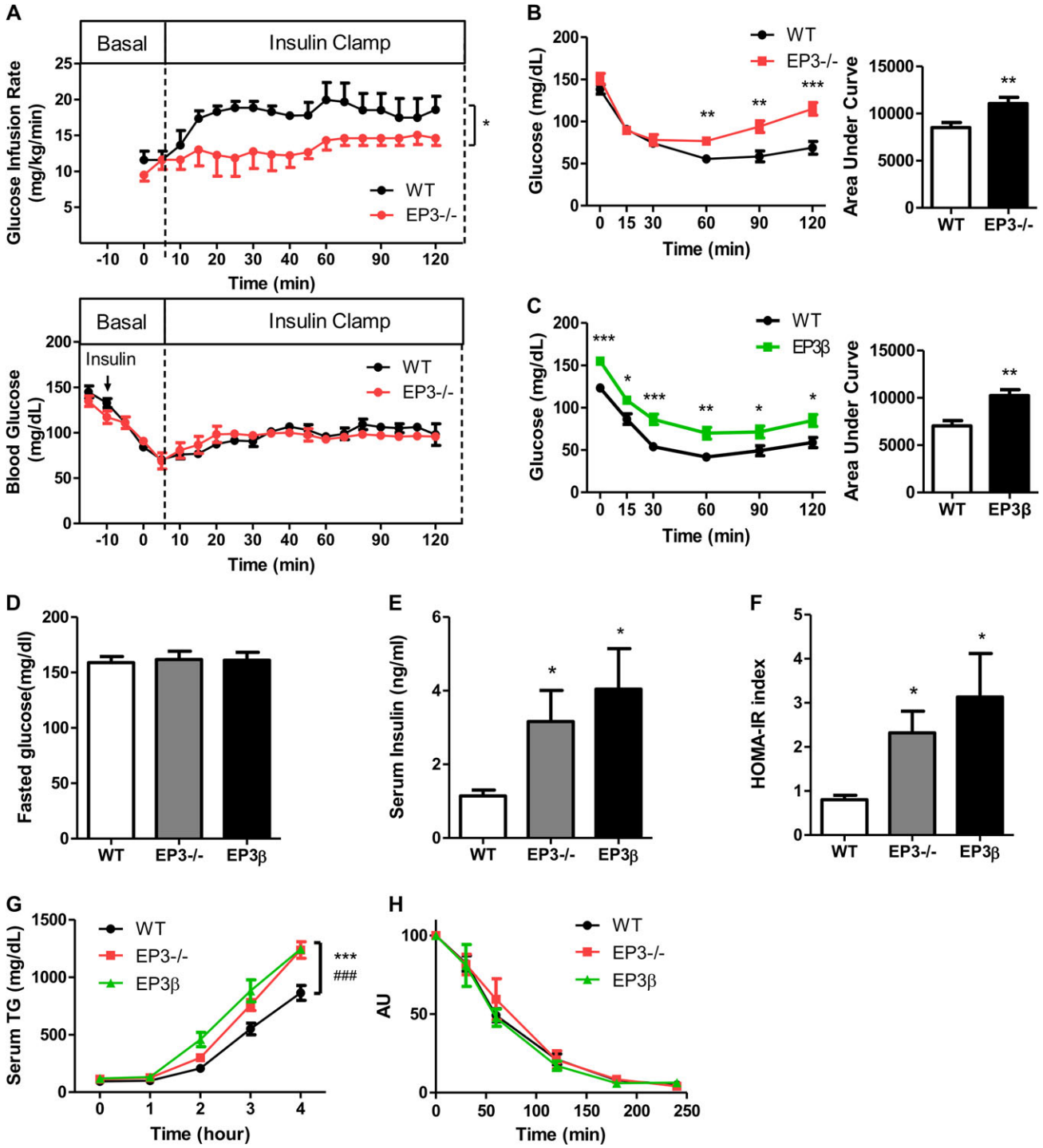

Figure 3 The EP3$^{-/-}$ and EP3β mice exhibited insulin resistance and enhanced VLDL-TG production. (**A** and **B**) The EP3$^{-/-}$ mice exhibited insulin resistance at 20 weeks. (**A**) Hyperinsulinemic-euglycemic clamp test of WT (n = 4) and EP3$^{-/-}$ (n = 3) mice. (**B**) ITT of WT (n = 15) and EP3$^{-/-}$ (n = 8) mice. (**C**) The EP3β mice exhibited insulin resistance at 20 weeks. ITT of WT (n = 17) and EP3β (n = 10) mice. (**D**–**F**) Determination of insulin resistant index in WT, EP3$^{-/-}$, and EP3β mice. Fasted plasma glucose (**D**) and insulin (**E**) of WT (n = 5), EP3$^{-/-}$ (n = 6), and EP3β (n = 5) mice were measured. (**F**) Insulin resistant index (HOMA-IR) was calculated with fasted plasma glucose concentration and insulin concentration. (**G**) Increased VLDL-TG production of EP3$^{-/-}$ and EP3β mice at 8 weeks. Serum TG was measured at different time points after intraperitoneal injection of tyloxapol. n = 8 for WT, n = 5 for EP3$^{-/-}$ mice, and n = 4 for EP3β mice. (**H**) No difference of TG clearance was observed among WT, EP3$^{-/-}$, and EP3β mice at 8 weeks. Serum TG was measured at different time points after tail vein injection of intralipid. n = 11 for WT, n = 7 for EP3$^{-/-}$ mice, and n = 5 for EP3β mice. AU, arbitrary unit. *P < 0.05, **P < 0.01, ***P < 0.001 vs. WT mice.

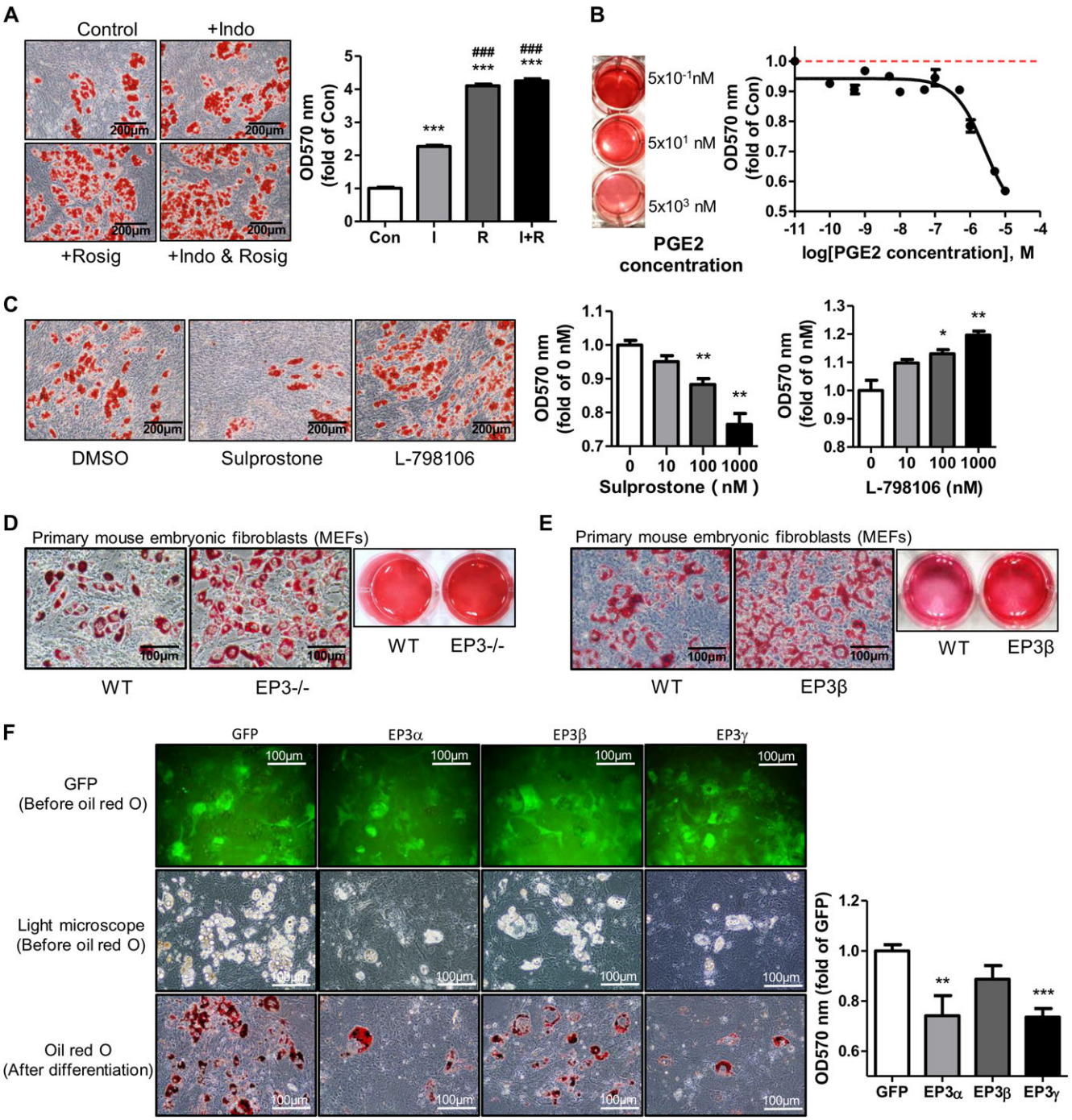

Figure 4 EP3 receptor suppressed preadipocyte differentiation. (**A**) Endogenous PGE2 inhibited MEF differentiation into adipocytes. MEFs were pretreated with 60 μM indomethacin for 1 h before the dexamethasone, IBMX, and insulin (DMI) induction with dexamethasone, insulin, and 3-isobutyl-1-methylxanthine (IBMX). Rosiglitazone was used as a positive control for adipogenesis. (**B**) Exogenous PGE2 inhibited adipogenesis. Different concentrations of exogenous PGE2 were used to treat WT MEFs before the DMI induction. (**C**) Effects of activation or blockade of EP3 on MEF differentiation. WT MEFs were pretreated with different concentrations of sulprostone or L-798106 for 1 h before the DMI induction. (**D**) Enhanced adipogenesis of the EP3$^{-/-}$ MEFs. MEFs from WT and EP3$^{-/-}$ embryos were cultured and differentiated. (**E**) Increased adipogenesis of the EP3β MEFs. MEFs from WT and EP3β embroys were cultured to differentiate into adipocytes. (**F**) The effect of each EP3 isoform on adipogenesis. EP3$^{-/-}$ MEFs were cultured and infected with the GFP, EP3α, EP3β, and EP3γ adenoviruses for 2 days before the DMI induction. For all adipogenesis experiments, after 8 days of differentiation, Oil Red O staining was performed, followed by taking images (**A** and **C** 200×, **D**–**F** 400×) or isopropanol dissolution. The absorption of dissolved Oil Red O was read under 570 nm wavelength. *$P < 0.05$, **$P < 0.01$, ***$P < 0.001$ vs. control (**A**, **C**) or GFP (**F**). $^{\#\#\#}P < 0.001$ vs. indomethacin (**A**). $n = 3$ for each group.

To determine whether EP3 receptor is involved in adipogenesis, MEFs were treated with sulprostone (an EP1 and EP3 agonist), L-798106 (a specific EP3 antagonist), or sc-19220 (a specific EP1 antagonist). As shown in Figure 4C, sulprostone significantly suppressed whereas L-798106 markedly facilitated MEF differentiation in a dose-dependent manner. However, sc-19220 treatment showed little effect on adipogenesis (Supplementary Figure S4B), indicating that sulprostone suppressed adipogenesis mainly through the activation of EP3 receptor rather than EP1 receptor. Similar effects were also observed in 3T3-L1 preadipocytes (Supplementary Figure S4C). However, sulprostone, L-798106, and DG-041 (another specific EP3 antagonist) had no effect on the differentiation of MEFs derived from EP3$^{-/-}$ (Supplementary Figure S4D) or EP3β (Supplementary Figure S4E) mice, further suggesting for the involvement of EP3 receptor, specifically EP3α and EP3γ isoforms but not EP3β isoform, in adipogenesis. Accordingly, terminal differentiation of the MEFs from both EP3$^{-/-}$ and EP3β mice to adipocytes were significantly enhanced compared to that of WT MEFs (Figure 4D and E). Similarly, primary preadipocytes from the epididymal fat of the EP3$^{-/-}$ mice exhibited increased ability to differentiate into adipocytes (Supplementary Figure S4F). To directly determine the role of each EP3 isoform in adipogenesis, GFP-tagged EP3α, EP3β, and EP3γ was put back individually to EP3$^{-/-}$ MEFs (Supplementary Figure S4G). Both EP3α and EP3γ dramatically suppressed the differentiation of EP3$^{-/-}$ MEFs, while EP3β had little effect (Figure 4F), further suggesting that the anti-adipogenic effect of EP3 receptor was mainly mediated by EP3α and EP3γ isoforms.

The role of the cAMP/PKA pathway in the anti-adipogenic effect of EP3 receptor

To characterize the signaling pathway underlying the regulation of adipogenesis by EP3 receptor, the expression of key genes and proteins involved in the adipogenic process was determined. Sulprostone suppressed the expression of key genes and proteins in the early (C/EBPβ) and late (PPARγ, C/EBPα, and AP2) stages of cell differentiation of MEFs or 3T3-L1 preadipocytes (Figure 5A, B and Supplementary Figure S5A, B). Furthermore, sulprostone suppressed the peroxisome proliferator response element (PPRE)-driven luciferase activity in WT MEFs but not in EP3$^{-/-}$ MEFs (Figure 5C). Intracellular contents of cAMP were significantly attenuated in response to sulprostone treatment when induced for differentiation in 3T3-L1 preadipocytes (Figure 5D). As expected, DMI-induced increase in phospho-Ser/Thr PKA substrate and phospho-CREB levels was markedly attenuated in sulprostone-treated 3T3-L1 preadipocytes (Figure 5E and Supplementary Figure S5C). In addition, the luciferase reporter assay using the pGL4.29 [luc2P/CRE/Hygro] Vector, a well-documented cAMP response element (CRE)-driven luciferase reporter, demonstrated that luciferase activity in both EP3$^{-/-}$ and EP3β MEFs was increased compared with WT MEFs, indicating an elevation of cAMP content in EP3$^{-/-}$ and EP3β MEFs (Figure 5F and G). Accordingly, dibutyryl cyclic AMP (dbcAMP), an analogue of endogenous cAMP, promoted the differentiation of primary preadipocytes isolated from WT mice and blocked the suppressive effect of sulprostone on adipogenesis (Supplementary Figure S5D). In contrast, H-89, an inhibitor of PKA, significantly suppressed the differentiation of primary preadipocytes isolated from EP3$^{-/-}$ mice (Supplementary Figure S5E), indicating that the inhibition of PKA abolished the enhanced adipogenesis caused by the removal of EP3 receptor. To determine the role of each EP3 isoform in intracellular cAMP production, pGL4.29 [luc2P/CRE/Hygro] reporter was transfected into EP3$^{-/-}$ MEFs in the presence of GFP, EP3α, EP3β, or EP3γ adenoviruses. EP3α induced the strongest inhibition on cAMP reporter luciferase activity, followed by EP3γ. The inhibition by EP3β was relative moderate but also significant (Figure 5H). Similarly, restoration of EP3α, EP3β, or EP3γ expression in EP3$^{-/-}$ MEFs resulted in decreased PKA activities, as measured by the phospho-Ser/Thr PKA substrate levels (Figure 5I). Consistently, sulprostone decreased whereas L-798106 increased cAMP reporter luciferase activity in WT and EP3β MEFs, but had no effect on EP3$^{-/-}$ MEFs (Supplementary Figure S5F).

Increased lipolysis in WAT of the EP3$^{-/-}$ and EP3β mice

It has been well documented that obese animals often display increased lipolysis and suffer from hyperlipidemia (Arner and Langin, 2014; Smith, 2015). Both EP3$^{-/-}$ and EP3β mice exhibited increased serum levels of glycerol and FFAs, with glycerol acting as an indicator of lipolytic activity in WAT (Supplementary Figures S2D and S6A, B). Consistently, primary mature adipocytes from EP3$^{-/-}$ and EP3β mice showed significantly enhanced lipolysis (Figure 6A, B). ATGL and HSL possess major TG hydrolase activities in adipose tissues. In both EP3$^{-/-}$ and EP3β mice, ATGL protein and phosphorylated HSL levels were significantly upregulated (Figure 6C, D and Supplementary Figure S6C, D). *In vitro* study found that the activation of EP3 receptor by sulprostone suppressed mRNA expression of ATGL and HSL during the differentiation of WT MEFs (Supplementary Figure S6E). As expected, sulprostone suppressed whereas L-798106 enhanced lipolysis in rat primary adipocytes in dose- and time-dependent manners, as reflected by the changes in glycerol concentration (Figure 6E and Supplementary Figure S6F–H). Furthermore, neither sulprostone nor L-798106 affected lipolysis in primary adipocytes from EP3$^{-/-}$ mice (Supplementary Figure S6I). Interestingly, sulprostone treatment in rat primary adipocytes significantly reduced cAMP contents and subsequent PKA activities, resulting in downregulation of phosphorylated HSL protein levels, with little effect on total HSL and ATGL protein expression (Figure 6F, G). The suppressive effect of sulprostone on lipolysis was reversed by forskolin, an adenylyl cyclase activator, or dbcAMP (Supplementary Figure S6J and K). Furthermore, PKA inhibitor H-89 completely abolished the lipolysis of primary adipocytes from EP3$^{-/-}$ mice (Supplementary Figure S6L). Together, these findings suggest that enhanced lipolysis in WAT of EP3$^{-/-}$ mice and EP3β mice was mediated through the cAMP/PKA signaling pathway.

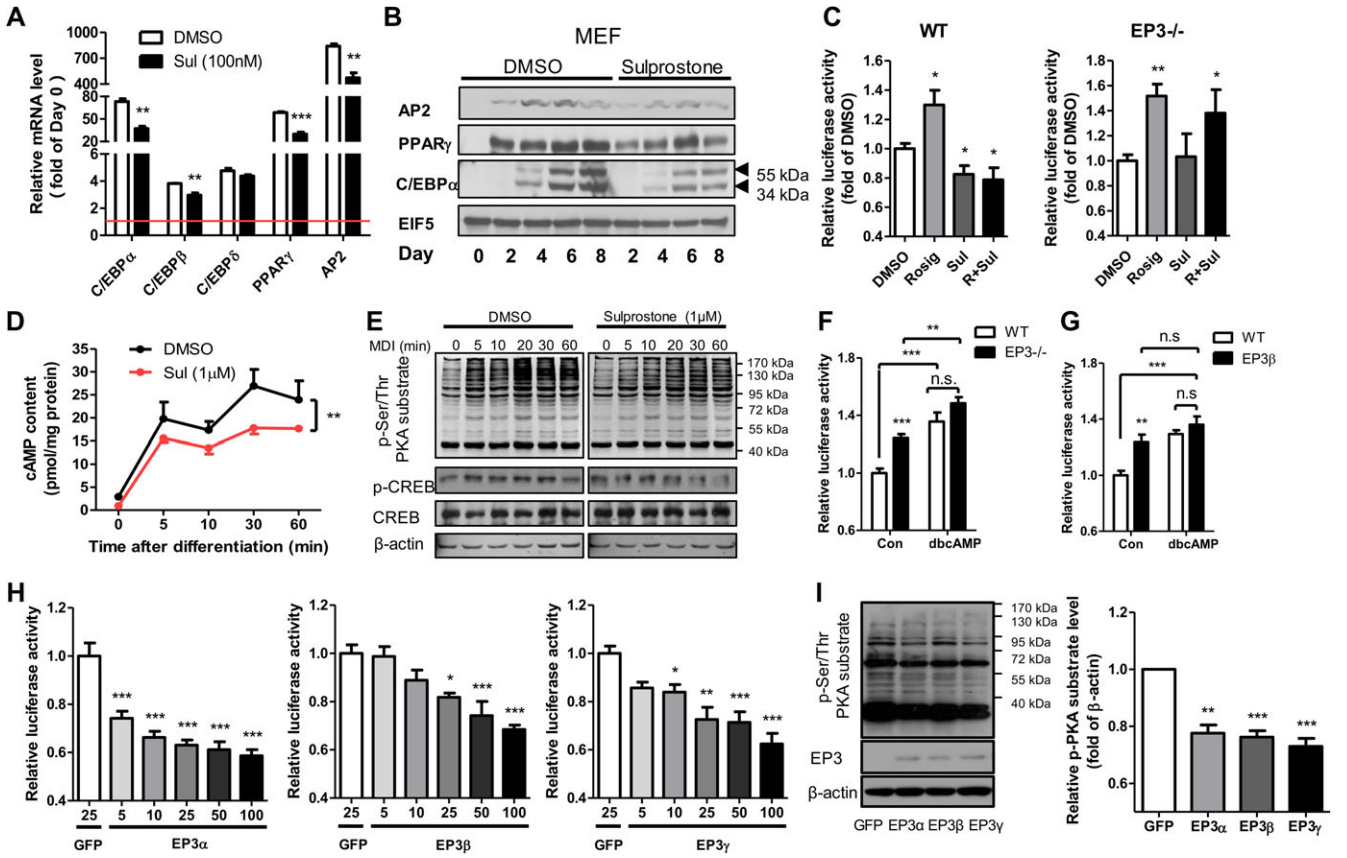

Figure 5 EP3 suppressed preadipocyte differentiation via the cAMP/PKA/PPARγ pathway. (**A**) The effect of sulprostone treatment on adipogenic gene expression. Pretreatment of WT MEFs with 100 nM sulprostone inhibited mRNA expression of preadipocyte differentiation markers on Day 4, as quantified by real-time PCR. Each gene was calculated by fold of Day 0 (the red line). (**B**) The effect of sulprostone treatment on adipogenic protein expression. Pretreatment of WT MEFs with 100 nM sulprostone decreased protein levels of AP2, PPARγ, and C/EBPα on different days. (**C**) Sulprostone suppressed the activity of PPARγ in WT MEFs. Relative PPRE-driven luciferase activity of WT and EP3$^{-/-}$ MEFs was tested, with 1 μM sulprostone treatment and 1 μM rosiglitazone as positive control. (**D** and **E**) Sulprostone inhibited DMI-induced activation of the cAMP/PKA pathway in 3T3-L1 cells. 3T3-L1 preadipocytes were pretreatment with 1 μM sulprostone. The cAMP content was measured by ELISA (**D**), and the phospho-Ser/Thr PKA substrate and phospho-CREB levels were detected by western blot (**E**). (**F** and **G**) Increased cAMP content in the EP3$^{-/-}$ and EP3β MEFs. Relative luciferase activity of WT and EP3$^{-/-}$ MEFs (**F**) or EP3β MEFs (**G**) were tested, with dbcAMP (0.5 mM) as positive control. (**H** and **I**) The effect of EP3α, EP3β, and EP3γ adenoviral infection on cAMP contents and PKA activity in EP3$^{-/-}$ MEFs. Relative CRE-driven luciferase activity of MEFs with the overexpression of EP3α, EP3β, and EP3γ, respectively, were tested (**H**). The phospho-Ser/Thr PKA substrate levels were detected by western blot (**I**). The right bargraph in **I** shows the quantification of western blots. For all adipogenesis experiments, after 8 days of differentiation, Oil Red O staining was performed, followed by taking images or isopropanol dissolution. The absorption of dissolved Oil Red O was read under 570 nm wavelength. *$P < 0.05$, **$P < 0.01$, ***$P < 0.001$ vs. DMSO (**A**, **C**, **D**), control (**F**, **G**), or GFP (**H**, **I**). $n = 3–4$ in each group.

Discussion

To date, little is known about the biological functions and signaling transduction of each EP3 isoform (Sugimoto and Narumiya, 2007). Sanchez-Alavez et al. (2007) reported that complete deletion of all EP3 isoforms in mice resulted in obese and insulin resistant phenotypes. However, the underlying mechanisms and the role of each EP3 isoform in WAT function remained uncharacterized. In the present study, we showed for the first time that EP3 receptor regulates both adipogenesis and lipolysis in mouse WAT, and disruption of all EP3 isoforms or EP3α/γ isoforms resulted in an obese phenotype associated with increased fat mass and insulin resistance.

PPARγ is considered as the master regulator of adipogenesis because it is not only necessary but also sufficient for this process (Rosen and MacDougald, 2006; Rosen and Spiegelman, 2014). We found that activation of EP3 receptor specifically suppressed PPARγ transcriptional activities and decreased PPARγ-driven expression of adipogenic genes. These findings may help explain the anti-adipogenic action of EP3 receptor. It has been previously reported that a moderate activation of the cAMP/PKA pathway leads to adipogenic induction (Gustafson et al., 2015). Naturally, EP3 receptor is mainly coupled to the Gi protein, resulting in the inhibition of adenylyl cyclase and reduction in cAMP levels (Hasegawa et al., 1996; Hizaki et al., 1997).

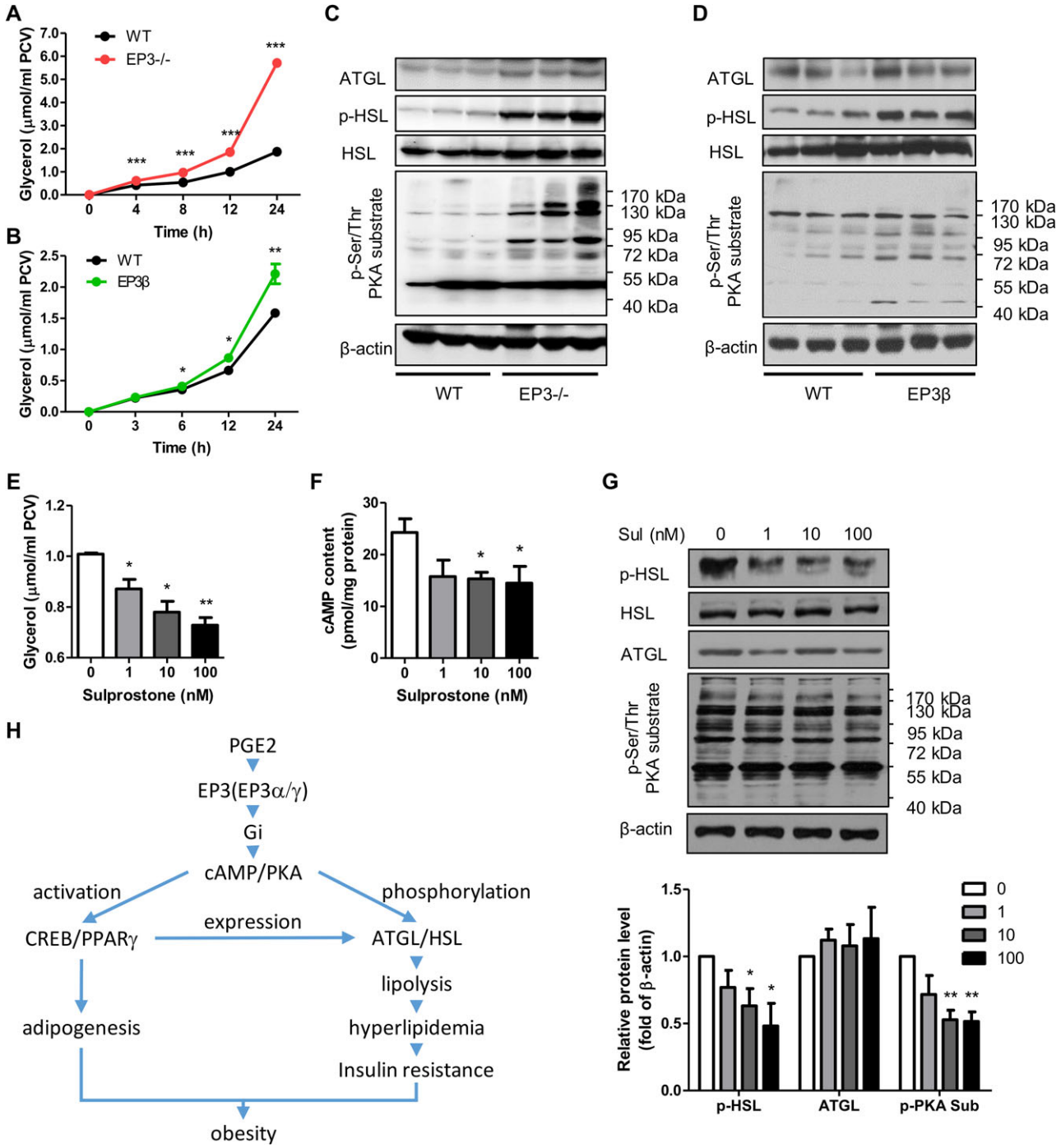

Figure 6 Increased lipolysis in WAT of the EP3$^{-/-}$ and EP3β mice. (**A**) Deletion of entire EP3 facilitated lipolysis. The glycerol was released into the medium from primary mature adipocytes of 12-week-old WT (n = 6) and EP3$^{-/-}$ (n = 6) mice at different time points. (**B**) Genetic ablation of both EP3α and EP3γ isoforms enhanced lipolysis. Primary mature adipocytes from 12-week-old WT (n = 4) and EP3β (n = 4) mice were cultured and the released glycerol was measured at different time points. (**C** and **D**) The effect of deletion of entire EP3 or EP3α and EP3γ isoforms on lipase expression and PKA activity. Protein levels of ATGL, HSL, phospho-HSL (Ser660), and phospho-Ser/Thr PKA substrate in the epididymal fat of WT and EP3$^{-/-}$ (**C**) or EP3β mice (**D**) were quantified by western blot. (**E**–**G**) The effect of sulprostone treatment on the cAMP/PKA/HSL pathway in rat primary mature adipocytes. Different concentrations of sulprostone were applied to rat primary mature adipocytes for 12 h. (**E**) The released glycerol was measured. (**F**) The cAMP content was determined by ELISA. (**G**) Protein levels of ATGL, HSL, phospho-HSL (Ser660), and phospho-Ser/Thr PKA substrate were detected by western bolt. The lower bargraph in **G** is the quantification of western blots. *P < 0.05, **P < 0.01, ***P < 0.001 vs. WT mice (**A**, **B**) or control (**E**–**G**). n = 3–4 in each group unless otherwise clarified. (**H**) An abridged view of EP3 in WAT and obesity.

We found that activation of EP3 receptor, especially its α and γ isoforms, suppressed the cAMP/PKA axis and decreased the differentiation of pre-adipocytes and MEFs to adipocytes. Thus, this may represent another mechanism for anti-adipogenic action of EP3 receptor.

All three EP3 isoforms appear to be functional in regulating intracellular cAMP levels and PKA activities, although EP3α and EP3γ seem to be two major isoforms mediating the anti-adipogenic effect of EP3. The cause(s) for different effects of three EP3 isoforms on adipogenic process by PKA activation are currently unknown. It has been previously reported that the three EP3 isoforms may also utilize distinct mechanisms to regulate PKA and ERK 1/2 activation (Namba et al., 1993; Israel and Regan, 2009), suggesting that EP3β may plays a different role within adipose tissue. Altogether, our study demonstrates that EP3α and EP3γ, but not EP3β, may be actively involved in regulating adipogenesis in WAT.

In the present study, we found that EP3$^{-/-}$ mice had more food intake and developed a spontaneous obese phenotype, which is consistent with a previous report that adult mice with complete deletion of all EP3 isoforms exhibit increased daytime feeding and an obese phenotype under a normal fat diet (Sanchez-Alavez et al., 2007). However, unlike previously reported, we also found that EP3$^{-/-}$ mice displayed less motor activity during both light and dark cycles, which is common behavior for most obese mammalians. In addition, we found that EP3β mice and EP3$^{-/-}$ mice exhibited similar weight gain and lipid accumulation, further supporting the possibility that EP3α and EP3γ play a predominant role in regulating preadipocytes differentiation in WAT *in vivo*.

Obesity is frequently associated with insulin resistance (Kahn and Flier, 2000). Increased lipolysis may be one of the factors contributing to obesity associated insulin resistance. In the present study, we found that both EP3$^{-/-}$ and EP3β mice exhibited increased lipolysis characterized by elevated plasma TG and glycerol levels before overt obese and insulin resistance. The enhanced lipolysis in EP3 receptor-deficient mice is likely due to increased levels of phosphorylated-HSL (p-HSL), a major active TG hydrolase in WAT. Increased p-HSL levels in WAT may result from marked PKA activation, a consequence of the inactivation of EP3 receptor. In addition, the expression of ATGL was also increased in WAT of both EP3$^{-/-}$ and EP3β mice. Although the mechanism by which EP3 receptor regulates HSL and ATGL expression and activity remains unclear, upregulation of PPARγ may play a role in this process, since activation of EP3 receptor significantly reduced PPARγ expression in preadipocytes. It has been previously reported that PPARγ controls the expression of ATGL and HSL (McTernan et al., 2002; Kershaw et al., 2007). Therefore, our results demonstrate that the deficiency of EP3 receptor promotes the lipase expression during the adipogenesis process and increases lipolysis in mature adipocytes via the cAMP/PKA/HSL pathway to elevate the activity of HSL. As a result of enhanced lipolytic activity in WAT of EP3$^{-/-}$ and EP3β mice, circulating FFA levels were increased, eventually leading to insulin resistance and ectopic lipid deposition in peripheral tissues including the liver (Arner and Langin, 2014).

Increasing evidence reveals that inflammation in WAT contributes to obesity and insulin resistance (Xu et al., 2003; Bastard et al., 2006). The present study demonstrates that both EP3$^{-/-}$ and EP3β mice exhibited increased inflammation in WAT, as reflected by upregulated phosphorylation of NF-κB, a transcription factor governing inflammatory process. However, the underlying mechanism by which EP3 receptor regulates NF-κB activity remains largely unknown.

In summary, as shown in Figure 6H, EP3 receptor is a vital Gi protein-coupled PGE2 receptor that inhibits adipogenesis via the cAMP/PKA/PPARγ pathway and blocks lipolysis mainly through the cAMP/PKA/HSL pathway in WAT. Inactivation or blockade of the entire EP3 receptor or EP3α and EP3γ isoforms results in adiposity and insulin resistance. Our study demonstrates that EP3 receptor is an important homeostatic factor in WAT. Our findings also identify a critical role of the PGE2/EP3 axis in bodily lipid and glucose metabolism.

Materials and methods

Chemicals and reagents

PGE2 and sulprostone were purchased from Cayman Chemical. Dimethyl sulphoxide (DMSO), indomethacin, L-798106, forskolin, dbcAMP, rosiglitazone, bovine insulin, 3-isobutyl-1-methylxanthine (IBMX), dexamethasone, tyloxapol, and intralipid were purchased from Sigma-Aldrich. EP3 receptor antibody (101760), ATGL antibody (10006409), AP2 antibody, and PPARγ antibody were from Cayman Chemical. C/EBPα antibody was from Santa Cruz. Antibodies against phospho-HSL (Ser660), HSL, phospho-Ser/Thr PKA substrate, p-NF-κB, NF-κB, p-AKT, and AKT were from Cell Signaling Technology. EP3α, EP3β, and EP3γ adenoviruses with GFP tags were generated using the pAdEASY-Track system and validated by gene sequencing and western blot analysis (Supplementary Figure S3G).

Experimental animals

Mice with genetic deletion of all EP3 isoforms (EP3$^{-/-}$ mice) or both EP3α and EP3γ isoforms (EP3β mice) were provided by Dr Richard M. Breyer at Vanderbilt University (Supplementary Figure S1). The mice were maintained on standard mouse chow and housed on a 12-h light–dark cycle under controlled temperature (22°C–24°C) and humidity (50%–65%) conditions in the animal facility of Peking University Health Science Center. Male EP3$^{-/-}$ and EP3β mice and sex- and age-matched WT littermates on a pure C57BL/6 background were used in all experiments. The study protocols and the use of the animals were reviewed and approved by the Animal Care and Use Review Committee of Peking University Health Science Center. The study conformed to the Guide for the Care and Use of Laboratory Animals published by the US National Institutes of Health (NIH publication no. 85–23, revised 1996). For details regarding the generation of the EP3$^{-/-}$ and EP3β mice, see Supplementary Materials and methods.

Recordings of mouse activity and food intake

Mice were continuously monitored for 24 h at 23°C in isolated metabolic chambers according to the instructions of the manufacturer (Harvard Apparatus) after acclimation for 1 day. Each cage was positioned on a custom-designed platform to measure animal locomotor activity. Daily food intake was calculated by measurement of consumed rodent chow (Lai et al., 2014).

MRI analysis

Total body fat and lean mass of EP3β and WT mice were measured without anesthesia or sedation using the EchoMRI™ device (Echo Medical Systems) (Lai et al., 2014).

Primary culture of mouse preadipocytes and MEFs

Preadipocytes were isolated from the epididymal fat tissue of 12-week-old WT and $EP3^{-/-}$ male mice. In brief, fat tissue was minced and digested with Type I collagenase dissolved in the Krebs-Ringer solution for 40–50 min. After digestion, preadipocytes were collected from stromal-vascular (SV) pellets after treatment with erythrocyte lysis solution for 5 min. The preadipocytes containing pellet was cultured in Dulbecco's Modified Eagle Medium (DMEM) with 10% fetal bovine serum (FBS) until growing to confluence for 2 days. For differentiation, preadipocytes were treated with 10% FBS and 0.5 mM IBMX, 1 μM dexamethasone, and 10 μg/ml insulin (DMI) for 2 days and then changed to 10% FBS-DMEM with insulin for another 2 days. For the next 4–8 days, large lipid droplets appeared in cells cultured with 10% FBS-DMEM medium. To isolate MEFs, 13.5-day WT, $EP3^{-/-}$, and EP3β embryos were collected. MEFs were plated in 6-well plate at 300000 cells/well. MEF differentiation was initiated 2 days after confluence with 10% FBS, 0.5 mM IBMX, 1 μM dexamethasone, 10 μg/ml insulin, and 1 μM rosiglitazone. From Day 3 to Day 8, cells were incubated with 10 μg/ml insulin, 1 μM rosiglitazone, and 10% FBS in DMEM.

Culture of primary adipocytes

Primary adipocytes were isolated from epididymal fat pads of normal male Sprague-Dawley rats (160–180 g) or 12-week-old mice as previously reported (Xu et al., 2009). The fat tissues were minced and digested in the Krebs-Ringer (pH = 7.4) solution containing 0.75 mg/ml Type I collagenase, 200 nM adenosine, 25 mM hepes, and 1% FFA-free BSA. After digestion, primary adipocytes floating in the tube were collected, washed, and packed by centrifugation at 200 × *g* for 3 min for determining the packed cell volume of adipocytes. Adipocytes were incubated in phenol red-free and serum-free DMEM in an atmosphere of 5% CO_2 at 37°C for 1 h before treatments.

Hyperinsulinemic euglycemic clamp, HOMA-IR measurement, and ITT

Hyperinsulinemic euglycemic clamp was performed as described previously (Brozinick et al., 2001; Tao et al., 2009). In brief, WT or $EP3^{-/-}$ mice were fasted for 6 h, and a hyperinsulinemic euglycemic clamp measurement was carried out with a prime-continuous infusion of human insulin at a rate of 60 pmol/kg/min. Blood samples were obtained every 10 min for determination of blood glucose concentration, which was controlled to the basal level (95 ± 5 mg/dl) by the perfusion of 10% glucose at variable rates for 2 h. The HOMA-IR index was calculated using the following formula: fasting glucose (mg/dl) × fasting insulin (U/ml)/405. For the ITT, mice were fasted for 4 h and then injected with insulin (0.75 U/kg) intraperitoneally. A drop of blood was taken from the tail vein before and after 15, 30, 60, 90, and 120 min injection of insulin for the determination of blood glucose with a glucometer. The total area under the glucose concentration curve was calculated using GraphPad Prism software.

Oil red O staining

To stain the differentiated MEFs or 3T3-L1 cells, 1 ml 4% paraformaldehyde was added for fixation for 10 min, and then 1 ml of Oil red O solution was added and incubated for another 10 min. After a few washes, 1 ml isopropanol was added to re-dissolve the Oil red O dye, and the absorbance at 570 nm was read. For liver sections, counterstaining with hematoxylin was performed after 10 min of Oil red O staining.

cAMP concentration analysis and the luciferase activity assay

The cAMP concentration was measured directly by the ELIAS kit (Cayman Chemical). The cAMP levels were also determined by the luciferase activity analysis of pGL4.29 [luc2P/CRE/Hygro] Vector (Promega) as previously described (Zhang et al., 2014). The cells were transfected with pGL4.29 [luc2P/CRE/Hygro] Vector and then infected with adenoviruses for 36 h. β-galactosidase reporter gene was co-transfected as a control for transfection efficiency. The cells were harvested and the luciferase activity was measured following the manual of assay kit (Promega). Luciferase activity of each sample was normalized to β-galactosidase activity. We used dbcAMP and/or forskolin as positive control. For PPRE-driven luciferase reporter and the non-adenovirus infected assay of pGL4.29 [luc2P/CRE/Hygro] Vector, the cells were transfected with the vector for 24 h and treated with drugs for 4 h, then the luciferase activity was measured.

Statistical analysis

GraphPad Prism software was used for statistical analysis. Data were evaluated by the analysis of variance (ANOVA) followed by Tukey *post hoc* tests or two-sided Student's *t*-test as appropriate and expressed as mean ± SE. $P < 0.05$ was required to reject the null hypothesis.

Supplementary material

Supplementary material is available at *Journal of Molecular Cell Biology* online.

Acknowledgements

We thank Mrs Mingfen Wei and Dr Huamin Wang from Peking University Health Science Center for their expert technical assistance. The experimental design of Dr Guoheng Xu from

Peking University Health Science Center is gratefully acknowledged. We also thank Prof. Fei Ye from the Institute of Materia Medica, Chinese Academy of Medical Sciences and Peking Union Medical College for technical assistance related to the hyperinsulinemic euglycemic clamp tests.

Funding

This work was supported by the National Basic Research Program of China (973 Program) (2012CB517504 to Y.-F.G.), the National Natural Science Foundation of China (81390351, 81270275, 81200511, and 81030003 to Y.-F.G.), National Institutes of Health grants (DK46205 to R.M.B.), the Swedish Research Council (to J.-A.G.), and Shenzhen Peacock Plan & JCYJ 20140418095735626.

Conflict of interest: none declared.

References

Ahmadian, M., Wang, Y., and Sul, H.S. (2010). Lipolysis in adipocytes. Int. J. Biochem. Cell Biol. *42*, 555–559.

Arner, P., and Langin, D. (2014). Lipolysis in lipid turnover, cancer cachexia, and obesity-induced insulin resistance. Trends Endocrinol. Metab. *25*, 255–262.

Bastard, J.P., Maachi, M., Lagathu, C., et al. (2006). Recent advances in the relationship between obesity, inflammation, and insulin resistance. Eur. Cytokine Netw. *17*, 4–12.

Bays, H. (2014). Central obesity as a clinical marker of adiposopathy; increased visceral adiposity as a surrogate marker for global fat dysfunction. Curr. Opin. Endocrinol. Diabetes Obes. *21*, 345–351.

Borglum, J.D., Pedersen, S.B., Ailhaud, G., et al. (1999). Differential expression of prostaglandin receptor mRNAs during adipose cell differentiation. Prostaglandins Other Lipid Mediat. *57*, 305–317.

Brozinick, J.T. Jr, McCoid, S.C., Reynolds, T.H., et al. (2001). GLUT4 overexpression in db/db mice dose-dependently ameliorates diabetes but is not a lifelong cure. Diabetes *50*, 593–600.

Dempersmier, J., and Sul, H.S. (2015). Shades of brown: a model for thermogenic fat. Front. Endocrinol. *6*, 71.

Fain, J.N., Leffler, C.W., Bahouth, S.W., et al. (2000). Regulation of leptin release and lipolysis by PGE2 in rat adipose tissue. Prostaglandins Other Lipid Mediat. *62*, 343–350.

Fujimori, K., Yano, M., Miyake, H., et al. (2014). Termination mechanism of CREB-dependent activation of COX-2 expression in early phase of adipogenesis. Mol. Cell. Endocrinol. *384*, 12–22.

Garcia-Alonso, V., and Claria, J. (2014). Prostaglandin E2 signals white-to-brown adipogenic differentiation. Adipocyte *3*, 290–296.

Gustafson, B., Hedjazifar, S., Gogg, S., et al. (2015). Insulin resistance and impaired adipogenesis. Trends Endocrinol. Metab. *26*, 193–200.

Hasegawa, H., Negishi, M., Ichikawa, A. (1996). Two isoforms of the prostaglandin E receptor EP3 subtype different in agonist-independent constitutive activity. J. Biol. Chem. *271*, 1857–1860.

Hizaki, H., Hasegawa, H., Katoh, H., et al. (1997). Functional role of carboxyl-terminal tail of prostaglandin EP3 receptor in Gi coupling. FEBS Lett. *414*, 323–326.

Israel, D.D., and Regan, J.W. (2009). EP(3) prostanoid receptor isoforms utilize distinct mechanisms to regulate ERK 1/2 activation. Biochim. Biophys. Acta *1791*, 238–245.

Jaworski, K., Ahmadian, M., Duncan, R.E., et al. (2009). AdPLA ablation increases lipolysis and prevents obesity induced by high-fat feeding or leptin deficiency. Nat. Med. *15*, 159–168.

Kahn, B.B., and Flier, J.S. (2000). Obesity and insulin resistance. J. Clin. Invest. *106*, 473–481.

Kershaw, E.E., Schupp, M., Guan, H.P., et al. (2007). PPARγ regulates adipose triglyceride lipase in adipocytes in vitro and in vivo. Am. J. Physiol. Endocrinol. Metab. *293*, E1736–E1745.

Kimple, M.E., Keller, M.P., Rabaglia, M.R., et al. (2013). Prostaglandin E2 receptor, EP3, is induced in diabetic islets and negatively regulates glucose- and hormone-stimulated insulin secretion. Diabetes *62*, 1904–1912.

Kimple, M.E., Neuman, J.C., Linnemann, A.K., et al. (2014). Inhibitory G proteins and their receptors: emerging therapeutic targets for obesity and diabetes. Exp. Mol. Med. *46*, e102.

Lafontan, M., and Langin, D. (2009). Lipolysis and lipid mobilization in human adipose tissue. Prog. Lipid Res. *48*, 275–297.

Lai, H., Jia, X., Yu, Q., et al. (2014). High-fat diet induces significant metabolic disorders in a mouse model of polycystic ovary syndrome. Biol. Reprod. *91*, 127.

Langin, D., and Arner, P. (2006). Importance of TNFα and neutral lipases in human adipose tissue lipolysis. Trends Endocrinol. Metab. *17*, 314–320.

Langin, D., Dicker, A., Tavernier, G., et al. (2005). Adipocyte lipases and defect of lipolysis in human obesity. Diabetes *54*, 3190–3197.

McTernan, P.G., Harte, A.L., Anderson, L.A., et al. (2002). Insulin and rosiglitazone regulation of lipolysis and lipogenesis in human adipose tissue in vitro. Diabetes *51*, 1493–1498.

Namba, T., Sugimoto, Y., Negishi, M., et al. (1993). Alternative splicing of C-terminal tail of prostaglandin E receptor subtype EP3 determines G-protein specificity. Nature *365*, 166–170.

Rosen, E.D., and MacDougald, O.A. (2006). Adipocyte differentiation from the inside out. Nat. Rev. Mol. Cell Biol. *7*, 885–896.

Rosen, E.D., and Spiegelman, B.M. (2014). What we talk about when we talk about fat. Cell *156*, 20–44.

Ryden, M., and Arner, P. (2007). Tumour necrosis factor-α in human adipose tissue – from signalling mechanisms to clinical implications. J. Intern. Med. *262*, 431–438.

Sanchez-Alavez, M., Klein, I., Brownell, S.E., et al. (2007). Night eating and obesity in the EP3R-deficient mouse. Proc. Natl Acad. Sci. USA *104*, 3009–3014.

Sanchez-Gurmaches, J., and Guertin, D.A. (2014). Adipocyte lineages: tracing back the origins of fat. Biochim. Biophys. Acta *1842*, 340–351.

Smith, U. (2015). Abdominal obesity: a marker of ectopic fat accumulation. J. Clin. Invest. *125*, 1790–1792.

Strong, P., Coleman, R.A., and Humphrey, P.P. (1992). Prostanoid-induced inhibition of lipolysis in rat isolated adipocytes: probable involvement of EP3 receptors. Prostaglandins *43*, 559–566.

Sugimoto, Y., and Narumiya, S. (2007). Prostaglandin E receptors. J. Biol. Chem. *282*, 11613–11617.

Tao, R., Ye, F., He, Y., et al. (2009). Improvement of high-fat-diet-induced metabolic syndrome by a compound from Balanophora polyandra Griff in mice. Eur. J. Pharmacol. *616*, 328–333.

Wang, C., Chen, Z., Li, S., et al. (2014a). Hepatic overexpression of ATP synthase β subunit activates PI3K/Akt pathway to ameliorate hyperglycemia of diabetic mice. Diabetes *63*, 947–959.

Wang, C., Chi, Y., Li, J., et al. (2014b). FAM3A activates PI3K p110α/Akt signaling to ameliorate hepatic gluconeogenesis and lipogenesis. Hepatology *59*, 1779–1790.

Xu, C., He, J., Jiang, H., et al. (2009). Direct effect of glucocorticoids on lipolysis in adipocytes. Mol. Endocrinol. *23*, 1161–1170.

Xu, H., Barnes, G.T., Yang, Q., et al. (2003). Chronic inflammation in fat plays a crucial role in the development of obesity-related insulin resistance. J. Clin. Invest. *112*, 1821–1830.

Ye, J. (2013). Mechanisms of insulin resistance in obesity. Front. Med. *7*, 14–24.

Zhang, X., Huang, S., Gao, M., et al. (2014). Farnesoid X receptor (FXR) gene deficiency impairs urine concentration in mice. Proc. Natl Acad. Sci. USA *111*, 2277–2282.